Nonsteroidal Anti-Inflammatory Drugs and Other Anthranilic Acids Inhibit the Na+/Dicarboxylate Symporter from Staphylococcus aureus

ARTICLE *in* BIOCHEMISTRY · APRIL 2013

Impact Factor: 3.02 · DOI: 10.1021/bi301611u

BIOCHEMISTRY
including biophysical chemistry & molecular biology

Article

pubs.acs.org/biochemistry

Nonsteroidal Anti-Inflammatory Drugs and Other Anthranilic Acids Inhibit the Na^+/Dicarboxylate Symporter from *Staphylococcus aureus*

Ana M. Pajor* and Nina N. Sun

Skaggs School of Pharmacy and Pharmaceutical Sciences, University of California—San Diego, La Jolla, California 92093-0718, United States

ABSTRACT: The Na^+/dicarboxylate symporter from *Staphylococcus aureus*, named SdcS, is a member of the divalent anion sodium symporter (DASS) family that also includes the mammalian SLC13 Na^+/dicarboxylate cotransporters, NaDC1 and NaCT. The mammalian members of the family are sensitive to inhibition by anthranilic acid derivatives such as *N*-(*p*-amylcinnamoyl)anthranilic acid (ACA), which act as slow inhibitors. This study shows that SdcS is inhibited by ACA as well as the fenamate nonsteroidal anti-inflammatory drugs, flufenamate and niflumate. The inhibition was rapid and reversible. The IC_{50} for ACA was approximately 55 μM. Succinate kinetics by SdcS were sigmoidal, with a $K_{0.5}$ of 9 μM and a Hill coefficient of 1.5. Addition of ACA decreased the V_{max} and increased the Hill coefficient without affecting the $K_{0.5}$, consistent with its activity as a negative modulator of SdcS activity. ACA inhibition was not correlated with the $K_{0.5}$ for succinate in SdcS mutants, and ACA did not affect the reactivity of the N108C mutant to the cysteine reagent, MTSET. We conclude that ACA and other anthranilic acid derivatives are effective allosteric inhibitors of SdcS. Furthermore, the mechanism of inhibition appears to be distinct from the mechanism observed in human NaDC1.

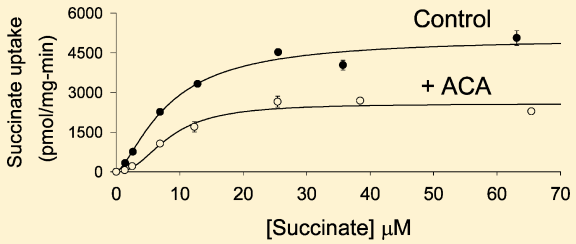

The Na^+/dicarboxylate symporter from *Staphylococcus aureus*, SdcS, is a member of the divalent anion sodium symporter (DASS) family that also includes the mammalian solute carrier 13 (SLC13) family.[1,2] The amino acid sequence of SdcS is approximately 35% identical to that of the mammalian SLC13 transporters, and its function is very similar. SdcS couples two Na^+ ions to the transport of four-carbon dicarboxylate substrates such as succinate, fumarate, and malate.[3,4] Very recently, the crystal structure of the Na^+/dicarboxylate transporter from *Vibrio cholerae*, VcINDY, also a DASS family member, was published.[5] The structure is in an inward-facing conformation with one sodium and one citrate molecule bound to the protein. The VcINDY protein fold is distinct from those of the neurotransmitter transporter and glutamate transporter families (LeuT and GltPH families, respectively), although there is a similar topology pattern of two halves related by inverse symmetry.[6]

The mammalian members of the SLC13/DASS family include three sodium-coupled transporters for dicarboxylates: NaDC1, NaDC3, and NaCT.[1] These plasma membrane transporters are important for absorbing divalent anion substrates, such as succinate or protonated citrate, from the plasma or renal tubular filtrate. The dicarboxylate transporters from the SLC13 family are all sensitive to inhibition by anthranilic acid derivatives, particularly *N*-(*p*-amylcinnamoyl)-anthranilic acid (ACA).[7] The K_i/IC_{50} for ACA is around 15 μM in human NaDC1.[7] ACA behaves as a slow and reversible inhibitor that produces a decrease in V_{max} without affecting K_m. The mammalian SLC13 transporters are also inhibited by fenamate-based nonsteroidal anti-inflammatory drugs (NSAIDs), including flufenamate and niflumate, although with very low affinity.[8] For example, the IC_{50} for flufenamate in hNaDC1 is ~2 mM.[8]

In this study, we examined inhibition of *S. aureus* SdcS by anthranilic acid derivatives. We found that most of the compounds that were tested inhibited the transport of succinate by SdcS, and the overall profile of inhibitors differed from that of human NaDC1. The most potent inhibitors of SdcS were ACA, Fmoc-anthranilic acid, and ONO-RS-082. The fenamate NSAIDS, flufenamate and niflumate, were also effective inhibitors. SdcS appeared to have an allosteric binding site for inhibitors, which act as negative modulators of transport, resulting in a decrease in V_{max} without affecting substrate affinity. Inhibition of the N108C mutant by ACA appeared to be independent of its inhibition by the cysteine reagent MTSET. We conclude that the dicarboxylate transporters of the DASS family, ranging from bacteria to humans, contain allosteric inhibitory binding sites for anthranilic acid derivatives. However, there appear to be differences in the mechanism or rate of inhibition in the bacterial and mammalian DASS transporters.

EXPERIMENTAL PROCEDURES

Preparation of Membrane Vesicles. *Escherichia coli* strain BL21 [F^- ompT hsdS_B(r_B^- m_B^-) gal dcm] (Lucigen) was used as a host for expression and function of plasmid-encoded pQE80L-SdcS.[3] This recombinant plasmid encodes SdcS with

Received: November 30, 2012
Revised: April 4, 2013
Published: April 8, 2013

   dx.doi.org/10.1021/bi301611u | *Biochemistry* 2013, 52, 2924−2932

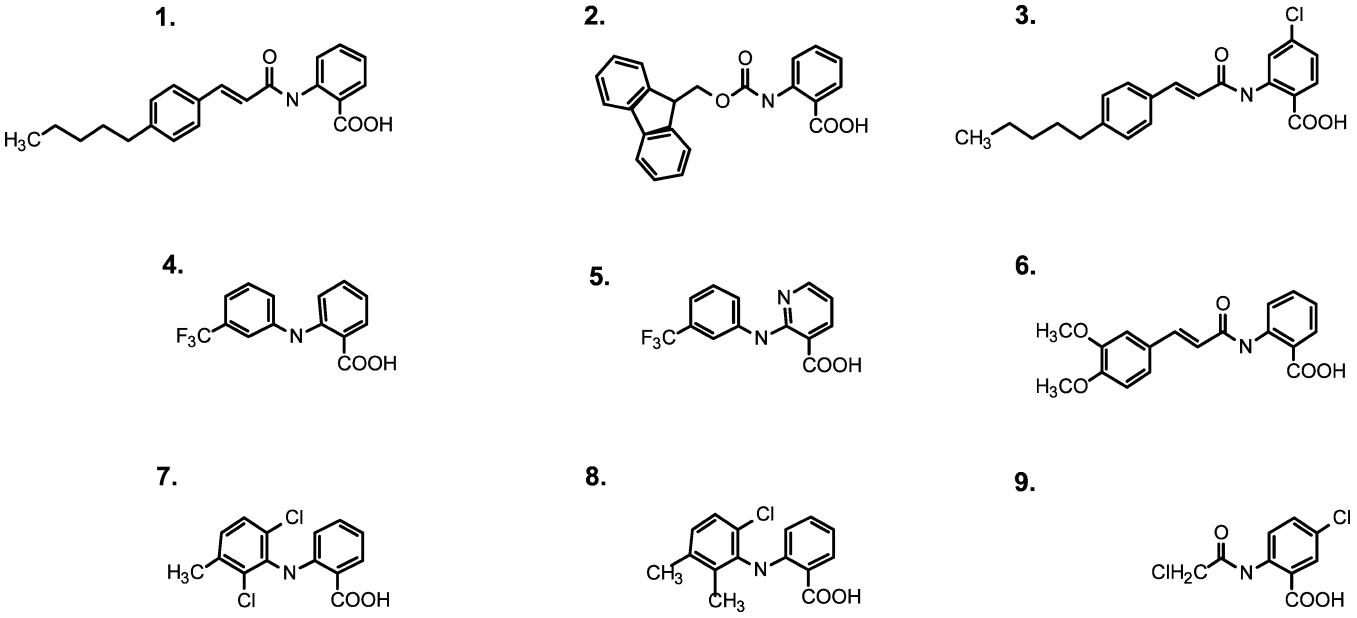

Figure 1. Structures of the compounds used in this study, listed in the order in which they are presented in Figure 2. The names of the compounds are listed in Table 1.

an N-terminal mRGS(H)$_6$GS amino acid extension and places SdcS expression under control of a T5 promoter/lac operator element. Overnight cultures of bacteria transformed with the SdcS plasmid were used to inoculate 500 mL of LB-Lennox broth (1:10 dilution) containing 50 μg/mL carbenecillin. Cells were grown at 37 °C to an optical density at 660 nm of 0.4–0.6. To induce SdcS expression, isopropyl β-D-galactopyranoside (IPTG) was added to a final concentration of 150 μM and cell growth was continued for an additional 2 h. Right-side-out (RSO) membrane vesicles from *E. coli* expressing SdcS were prepared as described previously.[9] Briefly, the washed cell pellets after IPTG induction were treated with DNase, RNase, and lysozyme followed by osmotic lysis with 50 mM potassium phosphate buffer (pH 6.6).[9] The membranes were then purified by differential centrifugation. RSO vesicles were resuspended in 100 mM potassium phosphate (KP_i) buffer (pH 7), frozen in liquid nitrogen, and stored at −80 °C.

Inside-out membrane vesicles (ISO) were also prepared as described previously.[9] Washed cell pellets after IPTG induction were treated with 0.5 mg/mL DNase and RNase and then passed through a French pressure cell (Thermo Scientific) at 4000 psi. Unbroken cells and organelles were removed by low-speed centrifugation at 10000*g* for 15 min at 4 °C. Membranes were sedimented by ultracentrifugation at 200000*g* for 45 min at 4 °C. Pellets containing crude ISO vesicles were resuspended in 100 mM KP_i buffer (pH 7.4) and further purified by sucrose density centrifugation at 27000 rpm (SW 32Ti rotor, Beckman) for 15 h at 4 °C. The sucrose density step gradient was prepared with 0.77, 1.44, and 2.02 M sucrose in 10 mM HEPES (pH 7.4). The upper band of membranes at the interface between 0.77 and 1.44 M sucrose was collected with a gradient collector and pelleted by ultracentrifugation at 200000*g* for 45 min at 4 °C. ISO membrane vesicles were resuspended in 100 mM KP_i buffer (pH 7.4), frozen in liquid nitrogen, and stored at −80 °C. Phenylmethanesulfonyl fluoride (PMSF, 0.5 mM) was added to all the steps to reduce the level of proteolysis.

Transport Assays. The uptake of [^{14}C]succinate by RSO and ISO membrane vesicles was performed by using a rapid filtration method, also as described previously.[9] Unless otherwise noted, the transport buffer contained 10 mM NaCl (final concentration), 90 mM choline chloride, and 50 mM MOPS, adjusted to pH 7 with 1 M Tris. Transport buffer (40 μL) containing 20 μM [^{14}C]succinate [specific activity of 62 mCi/mmol (Moravek Biochemicals)] was added to the bottom of a plastic tube (Falcon). A 10 μL drop of vesicles was added to the side of the tube, and the reaction was initiated by vortexing the two together. The final concentration of sodium was 10 mM. The reaction was stopped with 1 mL of ice-cold choline buffer [100 mM choline chloride and 50 mM MOPS (pH 7)], filtered immediately through a Millipore filter (0.45 μm pore size, type HAWP), and washed with 4 mL of ice-cold choline buffer. The radioactivity retained by the filters was measured by liquid scintillation counting.

For inhibition assays with ACA or other compounds, 40 μL of the vesicles was preincubated with 10 μL of an inhibitor stock solution for 10 min at room temperature. Inhibitor stock solutions were made in DMSO and then diluted in choline buffer before being added to the preincubation mixture. The final volume of DMSO in the transport reaction was 0.5%. Control solutions contained vehicle without inhibitor. The preincubation was followed by succinate transport assays in which 10 μL of pretreated vesicles was added to 40 μL of transport buffer containing [^{14}C]succinate and the same concentration of inhibitor as in the preincubation solution. The transport reaction was stopped with 1 mL of ice-cold choline buffer, as described previously. IC_{50} values were determined by fitting the data to a four-parameter logistic curve (SigmaPlot 10.0, Systat Software Inc.). For kinetic experiments, apparent kinetic constants for succinate transport were determined by fitting initial transport rates (10 s) to the Hill equation [$v = (V_{max}[S]^{n_H})/(K_{0.5}{}^{n_H} + [S]^{n_H})$, where [S] is the succinate concentration and n_H is the Hill coefficient] using nonlinear regression analysis (SigmaPlot version 10.0, Systat Software Inc.).

Transport Experiments with hNaDC1. The human NaDC1 transporter in the pcDNA3.1 plasmid was transiently

dx.doi.org/10.1021/bi301611u | *Biochemistry* 2013, 52, 2924–2932

expressed in COS-7 cells in 24-well plates, as described previously,[10] for initial screens of the inhibitors. Later IC_{50} measurements were done using HEK-293 cells, which have a higher level of expression of transfected hNaDC1, in 96-well white-sided Corning plates coated with poly-D-lysine. The HEK-293 cells were cultured in DMEM medium supplemented with 25 mM HEPES, 2 mM Glutamax, 1 mM sodium pyruvate, 0.1 mM nonessential amino acids, 10% heat-inactivated fetal calf serum, 100 units/mL penicillin, and 100 μg/mL streptomycin. The cells were transiently transfected using X-tremeGENE 9 (Roche) at a 3:1 ratio. Transport assays with [^{14}C]succinate were conducted 48 h after transfection, also as described previously.[7,10] Cells were dissolved using Ultima Gold scintillation cocktail (Perkin-Elmer), and then the plates were counted directly using a Wallac Microbeta plate scintillation counter. For all experiments, uptakes in vector-transfected cells were subtracted from uptakes in hNaDC1 plasmid-transfected cells to correct for background counts.

RESULTS

Inhibition of SdcS by Anthranilic Acids and/or Fenamates. Our previous study showed that the mammalian DASS/SLC13 transporters are sensitive to inhibition by anthranilic acid derivatives, particularly ACA.[7] Therefore, we tested the inhibition of succinate transport in the bacterial homologue, SdcS, using a similar series of anthranilic acid derivatives at 100 μM. The structures of the compounds used in this study are shown in Figure 1, and the names are listed in Table 1. As shown in Figure 2, all of the compounds tested inhibited SdcS transport activity. The strongest inhibition (shown by the lowest percent activity remaining after treatment with inhibitor) was seen with ACA, Fmoc-anthranilic acid, and ONO-RS-082, with <15% activity remaining. The fenamates, flufenamate and niflumate, produced intermediate inhibition, with <50% activity remaining. Tranilast, meclofenamate, and mefenamate treatment resulted in 56−71% activity remaining. Finally, 5-chloro-*N*-(2-chloroacetyl)anthranilic acid (5-chloro-AA) produced the smallest amount of inhibition, with ∼80% activity remaining.

Table 1. Compounds Used in This Study[a]

Number	Name
1	ACA, *N*-(*p*-amylcinnamoyl)anthranilic acid
2	*N*-Fmoc-anthranilic acid, *N*-(9-fluorenylmethoxycarbonyl) anthranilic acid
3	ONO-RS-082, *N*-(*p*-amylcinnamoyl)amino-4-chloroanthranilic acid
4	flufenamate, *N*-(3-trifluoromethylphenyl)anthranilic acid
5	niflumate, 2-[(3-trifluoromethyl)aniline]nicotinic acid
6	tranilast, *N*-(3′,4′-dimethoxycinnamoyl)anthranilic acid
7	meclofenamate, 2-[(2,6-dichloro-3-methylphenyl)amino]benzoic acid
8	mefenamate, 2-[(2,3-dimethylphenyl)amino]benzoic acid
9	5-chloro-AA, 5-chloro-*N*-(2-chloroacetyl)anthranilic acid

[a]The numbers refer to the structures shown in Figure 1.

ACA Inhibition and Time Course. ACA is a slow-onset inhibitor of human NaDC1, requiring preincubation for at least 3 min before inhibition can be detected and preincubation for at least 10 min for the full effect.[7] In contrast, the time course of the response of SdcS to ACA was very different (Figure 3A). Unlike the slow inhibition of the human transporter, the inhibition of SdcS by ACA appeared to be immediate, or at least within the 30 s time point used for the succinate transport assay. There was no difference in transport inhibition after different ACA preincubation times (Figure 3A). We also examined the reversibility of inhibition (Figure 3B). For this experiment, the vesicles were preincubated with and without ACA, and then the transport was measured in the presence or absence of added ACA. The addition of transport buffer containing [^{14}C]succinate resulted in a 5-fold dilution of the preincubation buffer, and the final concentration of ACA was either 40 μM (+ condition) or 8 μM (− condition). The level of transport of succinate by SdcS was reduced by ∼75% when ACA was present in both the preincubation and transport solutions (labeled +/+ in the figure). However, there was <10% inhibition of transport of succinate after dilution of the preincubation ACA to 8 μM (labeled +/− in the figure), indicating that the inhibition by ACA is rapidly reversible. Therefore, although the human and bacterial transporters bind ACA, the mechanism and rate of inhibition appear to be quite different.

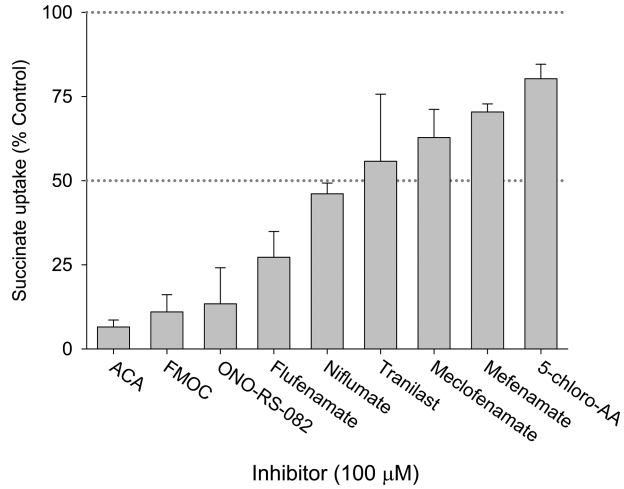

Figure 2. Inhibition of SdcS transport by anthranilic acid derivatives and NSAIDs. Transport of 20 μM [^{14}C]succinate was measured in the presence or absence of 100 μM inhibitor in right-side-out membrane vesicles expressing SdcS; 30 s uptakes were measured in transport buffer containing 10 mM sodium. Data are expressed as a percentage of control activity in the absence of inhibitor. Bars represent means ± the standard error of the mean (n = 3−5 separate membrane preparations). Dotted lines are shown at 50 and 100% activity. Abbreviations: FMOC, N-Fmoc-anthranilic acid; 5-chloro-AA, 5-chloro-*N*-(2-chloroacetyl)anthranilic acid.

Inhibitor Concentration Dependence. The concentration dependence of inhibition of [^{14}C]succinate transport in SdcS is shown in Figure 4. The experiments were repeated with at least two different batches of membrane vesicles. The IC_{50} values were 64 μM (Figure 4) and 47 μM (second experiment) for ACA, 57 μM (Figure 4) and 76 μM for ONO-RS-082, 51 μM (Figure 4) and 36 μM for Fmoc-anthranilic acid, and 84 μM (Figure 4) and 82 μM for flufenamate. In the experiment shown in Figure 4, the IC_{50} value for mefenamate was 70 μM and the inhibition was incomplete, with a maximal level of inhibition of ∼50%. In three experiments, the IC_{50} for mefenamate was 91 ± 9 μM and the maximal level of inhibition was 64 ± 9%. Note that the highest concentration of mefenamate that could be tested was 5 mM because of solubility problems.

dx.doi.org/10.1021/bi301611u | *Biochemistry* 2013, 52, 2924−2932

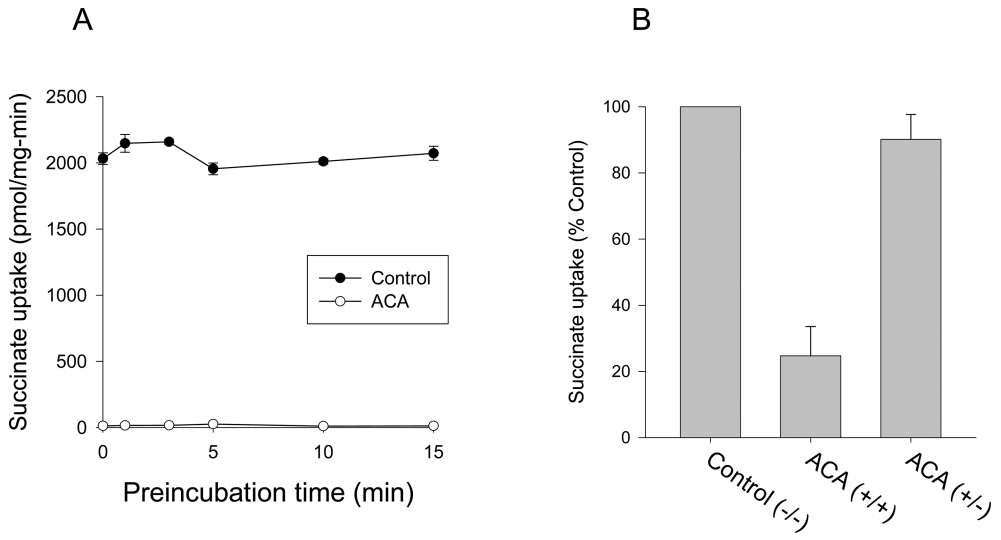

Figure 3. Time course and reversibility of ACA inhibition. (A) Time course. Transport of 20 μM [^{14}C]succinate was measured in right-side-out membrane vesicles expressing SdcS in the presence (ACA) or absence (control) of 100 μM ACA. Vesicles were preincubated with inhibitor or vehicle in choline buffer for up to 15 min, and then 30 s uptakes were measured in transport buffer containing 10 mM sodium. Data points represent means ± the range (n = 2 measurements from a single membrane preparation). (B) Reversibility. Transport of 20 μM [^{14}C]succinate was measured in right-side-out membrane vesicles expressing SdcS (as in panel A). The vesicles were preincubated for 10 min with 40 μM ACA or DMSO (indicated by the first + or −), followed by either ACA or DMSO in the transport solution (indicated by the second + or −). ACA (+/+) indicates ACA in both pre and transport solutions, and ACA (+/−) had only ACA in the preincubation solution. Data points represent means ± the range (n = 2 experiments with separate membrane preparations).

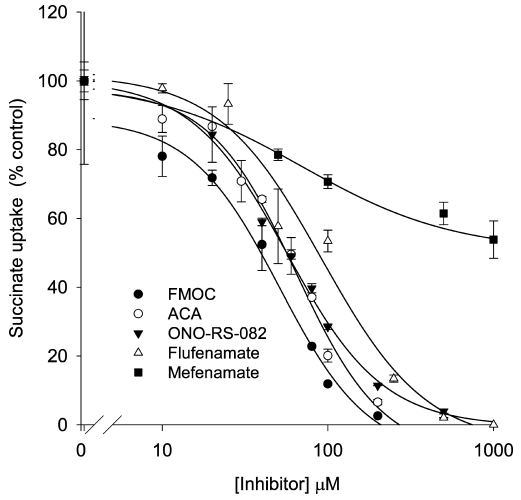

Figure 4. Concentration dependence of inhibition. Transport of 20 μM [^{14}C]succinate was measured for 10 s in right-side-out membrane vesicles expressing SdcS in the presence of different inhibitors. Mefenamate was tested up to 5 mM; all of the points were used for the curve fit, but only the data up to 1 mM are shown in the figure. The data shown are means ± the range (n = 2 measurements from a single membrane preparation). The IC_{50} values were 64 μM for ACA, 57 μM for ONO-RS-082, 51 μM for Fmoc-anthranilic acid, 84 μM for flufenamate, and 70 μM for mefenamate.

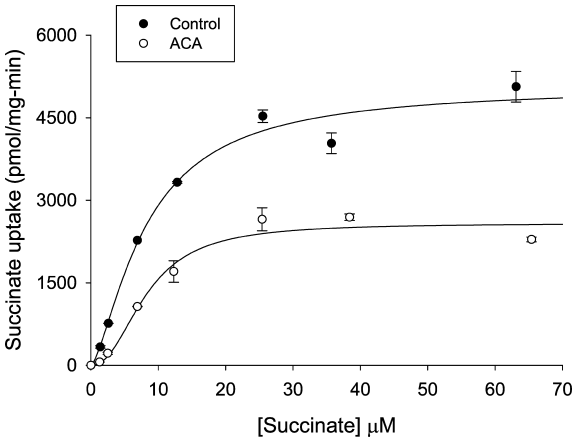

Figure 5. Effect of ACA on succinate kinetics by SdcS in RSO vesicles; 10 s uptake measurements of [^{14}C]succinate, in the presence and absence of 40 μM ACA, were measured in RSO vesicles expressing SdcS. The sodium concentration was 10 mM. Kinetic constants for succinate from this experiment for the control group were as follows: $K_{0.5}$ = 8.2 ± 1.4 μM, n_H = 1.46 ± 0.28, and V_{max} = 5071 ± 376 pmol mg^{-1} min^{-1} (mean ± standard error of the fit). In the presence of ACA, the kinetic constants were as follows: $K_{0.5}$ = 8.3 ± 1.1 μM, n_H = 2.25 ± 0.67, and V_{max} = 2582 ± 168 pmol mg^{-1} min^{-1}. The data points represent means ± the range (n = 2 measurements from a single membrane preparation).

Kinetic Effects of ACA Inhibition. The kinetics of succinate transport by SdcS were compared in paired experiments in the same vesicle preparations with and without ACA. Succinate kinetics by SdcS were sigmoidal and were analyzed using the Hill equation. In the experiment shown in Figure 5, the $K_{0.5}$ for succinate was 8.2 μM, the V_{max} was 5071 pmol mg^{-1} min^{-1}, and the Hill coefficient (n_H) was 1.46. In four experiments, the mean $K_{0.5}$ was 9.4 ± 1.5 μM, the V_{max} was 5768 ± 613 pmol mg^{-1} min^{-1}, and the Hill coefficient (n_H) was 1.52 ± 0.16 [mean ± standard error of the mean (SEM)]. In previous studies, we used the Michaelis−Menten equation to analyze succinate kinetics in SdcS,[9] but reanalysis of the same data using the Hill equation showed that the Hill coefficient was 1.41 ± 0.14 (n = 3). Addition of ACA to right-side-out membrane vesicles expressing SdcS changed both the V_{max} and the Hill coefficient, with no change in the $K_{0.5}$ for succinate. In the experiment shown in Figure 5, the $K_{0.5}$ in the presence of ACA was 8.3 μM, the V_{max} was 2582 pmol mg^{-1} min^{-1}, and the

dx.doi.org/10.1021/bi301611u | Biochemistry 2013, 52, 2924−2932

Hill coefficient (n_H) was 2.25. In three experiments with ACA present, the mean $K_{0.5}$ was 8.8 ± 0.6 μM and the Hill coefficient (n_H) was 2.48 ± 0.15 (mean ± SEM) . The normalized V_{max} in the presence of ACA was 37 ± 7% of the control (mean ± SEM; n = 3). Therefore, ACA appears to be a negative allosteric modulator of SdcS succinate transport.

ISO Vesicles. In some sodium-dependent transport proteins, the inhibitory binding site is located on one side of the membrane. For example, ibogaine inhibits the serotonin transporter when applied from the outside but not the inside of the cell.[11] Flufenamate, in contrast, has been shown to affect potassium channels from both the inside and the outside of the cell, possibly involving different mechanisms.[12] Therefore, we examined the inhibition of succinate transport by ACA in inside-out membrane vesicles (ISO) (Figure 6). If the binding site is more accessible from one side or the other, we would expect to see a difference in sensitivity. However, the inhibition by ACA in ISO vesicles was similar to that in RSO vesicles, with approximately 40% inhibition of transport by 50 μM ACA. ACA is membrane-permeant, and one possibility is that the inhibition would be slower if ACA had to diffuse across the membrane to its binding site. However, the preincubation time had no effect on succinate transport activity in ISO vesicles treated with 40 μM ACA: 42 ± 3.6% activity remaining (preincubation for 0 min) versus 40.9 ± 3.3% activity remaining (preincubation for 10 min) (mean ± SEM; n = 3 vesicle preparations; results not shown).

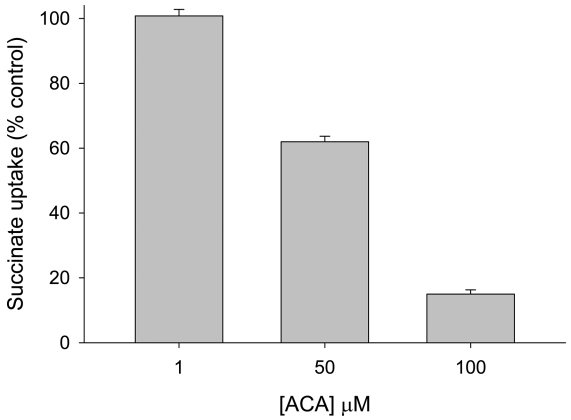

Figure 6. Inhibition of SdcS transport activity by ACA in ISO membrane vesicles. ISO vesicles were preincubated with vehicle (control) or 1, 50, or 100 μM ACA for 10 min. Transport uptake of 20 μM [^{14}C]succinate was then measured for 30 s in buffer containing 10 mM sodium. The results are expressed as a percentage of control, incubated with vehicle only. Bars represent means ± SEM (n = 3 separate membrane preparations).

Inhibition of SdcS Mutants by ACA. We next examined the effect of ACA on SdcS mutants. We found previously that wild-type SdcS and the C457S and N108C/C457S mutants have similar K_m values for succinate.[9] However, the L436C/C457S mutant has a higher K_m value.[9] The single endogenous cysteine in SdcS at position 457 is not required for function, and the K_m for succinate in the C457S mutant is similar to that of the wild type.[9] However, the C457S mutant appeared to be less sensitive to inhibition by ACA (Figure 7A). The N108C/C457S double mutant was similar to C457S, but L436C/C457S restored the ACA sensitivity to that of the wild type (Figure 7B). Overall, the ACA sensitivity was not correlated with the K_m for succinate, in agreement with the kinetic findings that ACA affects V_{max} rather than substrate affinity.

The cysteine mutants were originally prepared for experiments involving the membrane-impermeant cysteine reagent, MTSET.[9] Our previous study showed that the N108C/C457S double mutant was sensitive to inhibition by MTSET in both RSO and ISO vesicles, whereas the L436C/C457S mutant was not affected.[9] Therefore, we examined whether ACA could affect the sensitivity of N108C/C457S to MTSET. There was no difference in the dose response to MTSET in the presence or absence of 40 μM ACA (Figure 7B), with average IC_{50} values for MTSET of 44 ± 17 μM (without ACA) and 37 ± 1 μM (with ACA) (n = 2 experiments). The pseudo-first-order rates of inactivation calculated from the IC_{50} values[13] were 1.85 ± 0.71 min^{-1} mM^{-1} (no ACA) and 1.90 ± 0.03 min^{-1} mM^{-1} (with ACA). Therefore, the effect of ACA on N108C/C457S appears to be independent of the effect of MTSET. Interestingly, the maximal level of inhibition by MTSET in this study was ~65%. In contrast, our previous study showed approximately 90% inhibition of N108C/C457S by MTSET at 1 mM.[9]

Human NaDC1. Our previous study with human NaDC1 in a continuous cell line did not examine all of the inhibitors tested in the study presented here. For comparison with the bacterial transporter, we tested the same inhibitors against human NaDC1 using transiently transfected cells (Figure 8A). The K_m for succinate in hNaDC1 is ~1.1 mM, and the IC_{50}/K_i for ACA is ~15 μM.[7,10] In this study, inhibition of hNaDC1 by 100 μM ACA, Fmoc-anthranilic acid, and ONO-RS-082 was similar to what we observed previously.[7] There was no inhibition by flufenamate at 100 μM (Figure 8A). Interestingly, there was consistent stimulation of succinate transport by niflumic acid. It is not clear if this was a direct effect on the transporter or indirect, possibly related to inhibition of endogenous chloride channels by niflumate.[14] There was a slight inhibition (approximately 13%) by 5-chloro-AA at 100 μM. Finally, there was no transport inhibition by the other compounds tested: tranilast, meclofenamate, and mefenamate (Figure 8A).

The concentration dependence of some of these inhibitors on hNaDC1 transport is shown in Figure 8B. The IC_{50} for ACA was 9 μM (shown in Figure 8B), and the mean of three experiments was 7.7 ± 2.5 μM (mean ± SEM), consistent with our previous results. The IC_{50} for ONO-RS-082 was 26 μM (Figure 8B), and the mean of three experiments was 26 ± 6 μM. The IC_{50} for Fmoc-anthranilic acid was 125 μM (Figure 8B), and the mean of three experiments was 142 ± 51 μM. Finally, the IC_{50} for flufenamate was 830 μM (Figure 8B), and the mean of four experiments was 1303 ± 320 μM, similar to the results of previous experiments using the *Xenopus* oocyte expression system.[8]

■ DISCUSSION

Anthranilic acid derivatives, such as ACA, have been shown to inhibit the mammalian SLC13 dicarboxylate transporters, NaDC1, NaDC3, and NaCT.[7] The sequence of the Na$^+$/dicarboxylate symporter, SdcS, from *S. aureus* is approximately 35% identical to those of the mammalian SLC13 transporters and has a similar sodium-coupled transport mechanism. The main finding of our study is that succinate transport by SdcS is also inhibited by ACA and other anthranilic acids, including the NSAIDs, flufenamate, and niflumate. Furthermore, the

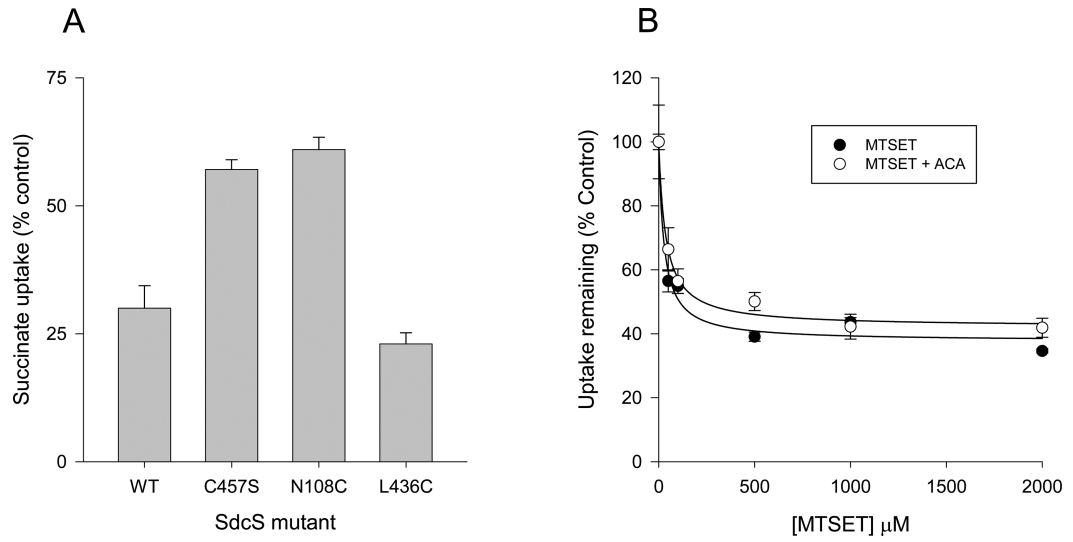

Figure 7. (A) Inhibition of succinate transport by ACA in wild-type and mutant SdcS. The N108C and L436C mutants were made in a C457S background. Right-side-out membrane vesicles were treated with 40 μM ACA or vehicle for 10 min, and then transport of 20 μM [^{14}C]succinate was measured for 30 s in buffer containing 10 mM sodium. The transport activity is expressed as a percentage of control without ACA. The bars represent means ± SEM (n = 3 separate membrane preparations). (B) Effect of ACA on inhibition of succinate transport by MTSET in the N108C mutant. RSO vesicles expressing N108C were preincubated for 10 min with increasing concentrations of MTSET (0−2000 μM) with or without 40 μM ACA. Transport of 20 μM [^{14}C]succinate was measured for 30 s. The data are shown as a percentage of the control without MTSET. The addition of ACA inhibited transport by 71.2%.

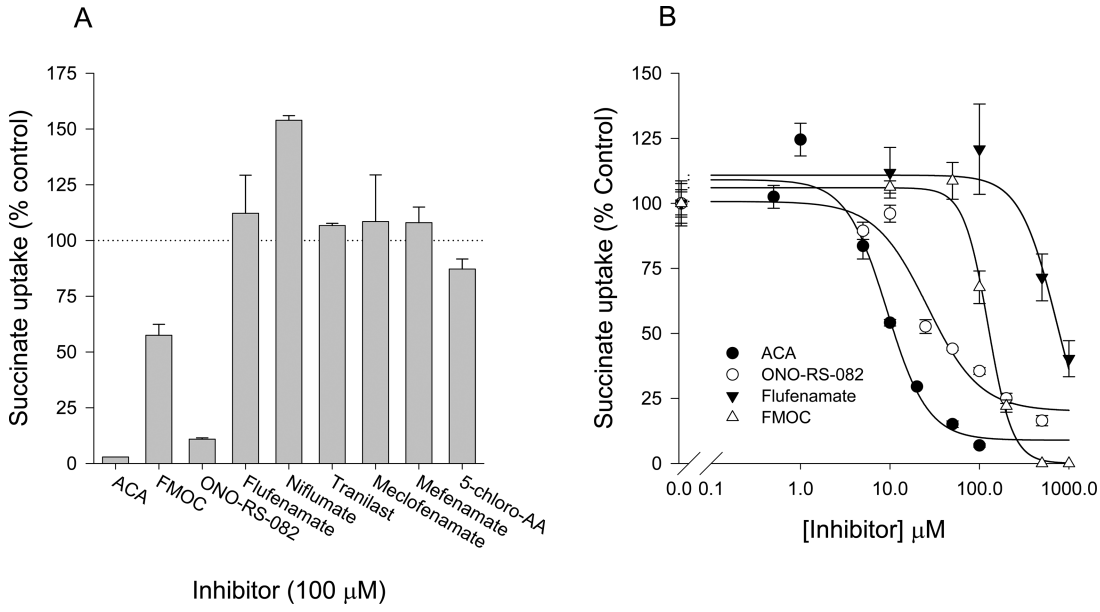

Figure 8. (A) Inhibition of human NaDC1 by anthranilic acids. The cells transfected with the hNaDC1 plasmid were preincubated with inhibitor for 10 min, followed by 30 min uptakes using 10 μM [^{14}C]succinate. The inhibitors are listed in the same order as in Figure 2, and the results are expressed as a percentage of the control without inhibitor. Note that niflumic acid consistently stimulated transport. The bars represent means ± the range (n = 2 separate experiments). (B) Succinate transport activity by hNaDC1 at increasing inhibitor concentrations. The data were normalized to transport activity without inhibitor (control, 100%). The bars represent means ± SEM (n = 3 wells from a single experiment). Flufenamate was tested up to 10 mM; all of the points were used for the curve fit, but only the data up to 1 mM are shown. The IC_{50} values were 9 μM for ACA, 26 μM for ONO-RS-082, 125 μM for Fmoc-anthranilic acid, and 830 μM for flufenamate.

mechanism of inhibition may be slightly different in the bacterial and mammalian transporters.

SdcS was inhibited by a wide range of anthranilic acids, with some inhibition by all of the compounds tested in this study. The IC_{50} values for ACA, ONO-RS-082, and Fmoc-anthranilic acid were all approximately 40−60 μM, whereas the IC_{50} for flufenamate was ∼80 μM. Mefenamate had a similar IC_{50} of ∼90 μM, but it did not completely inhibit succinate transport by SdcS. In contrast, human NaDC1 was more sensitive to inhibition by ACA, with an IC_{50} of 8 μM in this study and IC_{50}/K_i values of approximately 15 μM in our previous study.[7] The IC_{50} for flufenamate in hNaDC1 was much higher, ∼1.3 mM in this study and 2 mM in hNaDC1 expressed in *Xenopus* oocytes.[8] The inhibitor IC_{50} values were not related to the relative succinate affinities in the two transporters, with a $K_{0.5}$ for succinate of 9 μM in SdcS compared with a K_m of 590 μM

dx.doi.org/10.1021/bi301611u | *Biochemistry* 2013, 52, 2924−2932

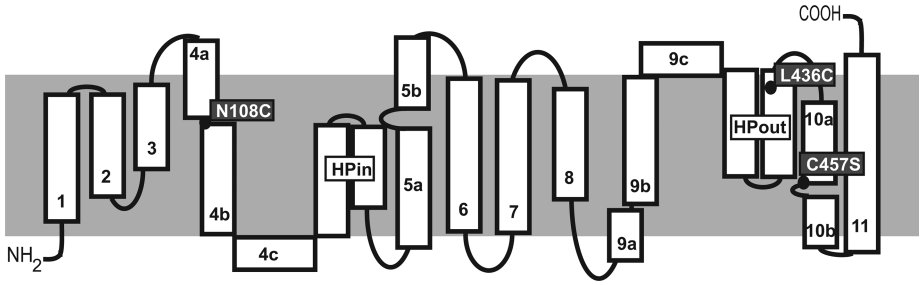

Figure 9. Secondary structure model of SdcS, based on the vcINDY crystal structure.[5] The cytoplasmic side is at the bottom of the figure. The positions of mutated residues from this study (N108C, L436C, and C457S) are shown as solid dots. The substrate and cation binding residues are located primarily in HP_{in} and TM 5 at the N-terminus and in HP_{out} and TM 10 at the C-terminus.[5]

in hNaDC1.[10] Another important difference between the bacterial and mammalian transporters is the fact that the onset of inhibition and reversibility was very rapid in SdcS but required preincubation or postincubation for several minutes in hNaDC1.[7]

In this study, the inhibition of succinate transport by ACA reduced the V_{max} for transport without affecting $K_{0.5}$, consistent with a negative allosteric modulator. It was somewhat surprising that the inhibition by ACA occurred from either side of the membrane, in both RSO and ISO vesicles regardless of preincubation time. However, this could indicate that there is an alternately accessible binding site located on the opposite side of the membrane from the substrate binding site and there is rapid diffusion of the inhibitor across the membrane. Another possibility is a single fixed inhibitor binding site, but inhibitor diffusion allows rapid inhibition when applied from the other side of the membrane. ACA is a nonspecific phospholipase A2 inhibitor that is membrane-permeant,[15] so diffusion to an inhibitory site on the opposite side of the membrane from the substrate binding site would be possible. A less likely explanation for the effects of ACA is that different mechanisms mediate the effects from each side of the membrane. As an example, flufenamate inhibits I_AK^+ channels from both sides of the membrane, although the effects seen on the inside of the cell may be indirect through modulation of cyclooxygenase activity.[12] However, an indirect inhibition mechanism is not as likely for SdcS because the assays were conducted using purified membrane vesicles.

There are several well-characterized examples of transporters that contain allosteric inhibitory sites. For example, the GLUT1 glucose transporter is inhibited by cytochalasin B, which binds at or near the glucose efflux site on the inside of the membrane. Cytochalasin B inhibition kinetics are noncompetitive upon examination of influx, but competitive upon examination of efflux or equilibrium exchange.[16,17] Similarly, bongrekik acid inhibits the mitochondrial ADP/ATP exchanger by diffusing across the membrane and binding to the inward-facing conformational state of the protein.[18] The LeuT leucine transporter, a bacterial homologue of the neurotransmitter transporter family (SLC6), contains an allosteric inhibitor site that binds tricyclic antidepressants and is accessible from the outside of the cell.[19,20] Crystal structures of LeuT show that the antidepressant molecules bind in a vestibule separate from the two Na^+ ions and substrate.[19,20] The structures suggest that inhibition by antidepressants occurs via stabilization of the external gate of LeuT, which prevents the intracellular release of cations and substrate.

The recent crystal structure of a DASS family transporter, VcINDY from *Vibrio cholerae,* is in an inward-facing conformation.[5] The protein has an inverted repeat structure, with the substrate binding site consisting of residues from both halves of the protein. At present, there is no information about the possible location of the inhibitory binding site in the DASS/SLC13 family, but it is likely that the site is distinct from the substrate or cation binding sites. Figure 9 shows the secondary structure model of SdcS, based on the VcINDY structure. The substrate and cation binding residues in the VcINDY structure are primarily located in the unwound helices from the hairpin loop, HP_{in}, and between TM 5a and TM 5b at the N-terminal half of the protein, and in HP_{out} and between TM 10a and TM 10b in the C-terminal half of the protein.[5] The single endogenous cysteine at position 457 in SdcS is predicted to be located between TM 10a and TM 10b (Figure 9). Cys457 is accessible to membrane-impermeant cysteine-specific reagents from the inside of the cell, and the C457S mutation does not affect substrate kinetics.[9] This study showed that the sensitivity of C457S to inhibition by ACA was decreased compared with that of wild-type SdcS, and the L436C/C457S double mutant restored the ACA sensitivity to wild-type levels, suggesting that the ACA binding site is located near these residues. The N108C mutant, located in the unwound portion of TM 4, had ACA sensitivity similar to that of C457S. Furthermore, the presence of ACA did not alter the reactivity of N108C to MTSET, indicating that the inhibition by ACA occurs in a manner that is independent of the inhibition by MTSET at position 108. Taken together, these results support the hypothesis that at least part of the ACA binding domain is located near the carboxy-terminal portion of the protein, possibly around HP_{out} and TM 10a and TM 10b.

Succinate transport by SdcS exhibited sigmoid kinetics, with an apparent Hill coefficient of ~1.5. This suggests that SdcS contains at least two succinate binding sites that exhibit moderate cooperativity.[21] Our previous kinetic experiments with SdcS did not appear to be obviously sigmoidal and were analyzed using the Michaelis−Menten equation. Reanalysis of the data showed Hill coefficients of 1.62 ± 0.18 in intact cells[3] and 1.42 ± 0.2 in right-side-out membrane vesicles.[9] However, in proteoliposomes, the SdcS succinate kinetics were more hyperbolic, with a mean Hill coefficient of 0.83 ± 0.02.[4] It is possible that SdcS contains a second substrate binding site, which may or may not be evident in the kinetics, possibly depending on the conditions. An alternate explanation is that the two substrate binding sites are found on separate SdcS proteins that form a dimer. The VcINDY protein forms a dimer in the crystal structure with both protomers oriented in the same direction,[5] although there is no information about whether the dimer is the functional unit. There is precedence for transporters with multiple interacting subunits as well as

dx.doi.org/10.1021/bi301611u | *Biochemistry* 2013, 52, 2924−2932

allosteric substrate binding sites. For example, the GLUT1 glucose transporter is a tetramer (a dimer of dimers) with two interacting sugar binding sites.[22] The carnitine/butyrobetaine antiporter (CaiT) has an allosteric regulatory substrate binding site on the same protein, and this site needs to be occupied to initiate substrate translocation.[23] The Na^+/leucine transporter (LeuT), a neurotransmitter transporter homologue, may also contain an allosteric regulatory substrate binding site, although this is still being debated.[24] In one study, the detection of the second high-affinity substrate binding site in LeuT was dependent on the conditions used to prepare the samples.[25]

In addition to sigmoidal succinate kinetics in SdcS, inhibition of succinate transport by ACA resulted in a decreased V_{max} and an increased Hill coefficient, without affecting substrate affinity. The kinetic effect of ACA is consistent with noncompetitive inhibition, involving an allosteric inhibitor binding site that is distinct from the substrate binding site. Depending on the mechanism of inhibition, it is not unusual for an inhibitor to produce increased apparent cooperativity, as shown by an increased Hill coefficient.[21] One possible mechanism of the effect of ACA could be a reduction in the proportion of transporters with a conformational state that allows substrate binding.[21] Alternatively, it is possible that binding of ACA to SdcS stabilizes a conformation that has a lower transport activity or that prevents substrate binding or release. Our current working model is one in which SdcS contains at least two interacting substrate binding sites, and an allosteric inhibitor binding site that may be located on the opposite side of the membrane from the substrate binding site. We conclude that anthranilic acids are effective inhibitors of the members of the DASS family, although there are differences in the rate or mechanism of inhibition between the bacterial and mammalian transporters.

AUTHOR INFORMATION

Corresponding Author

*Skaggs School of Pharmacy and Pharmaceutical Sciences, University of California—San Diego, La Jolla, CA 92093-0718. Phone: (858) 822-7806. Fax: (858) 822-5591. E-mail: apajor@ucsd.edu.

Funding

This work was supported by National Institutes of Health Grant DK46269.

Notes

The authors declare no competing financial interest.

ACKNOWLEDGMENTS

Thanks to Shelly Peng and Ereca Nguyen for their assistance in making solutions and media.

ABBREVIATIONS

ACA, *N*-(*p*-amylcinnamoyl)anthranilic acid; MTSET, [2-(trimethylammonium)ethyl]methanethiosulfonate; SdcS, sodium dicarboxylate symporter; DASS, divalent anion sodium symporter; SLC13, solute carrier family 13; NSAIDs, nonsteroidal anti-inflammatory drugs.

REFERENCES

(1) Pajor, A. M. (2006) Molecular properties of the SLC13 family of dicarboxylate and sulfate transporters. *Pfluegers Arch. 451*, 597−605.

(2) Prakash, S., Cooper, G., Singhi, S., and Saier, M. H., Jr. (2003) The ion transporter superfamily. *Biochim. Biophys. Acta 1618*, 79−92.

(3) Hall, J. A., and Pajor, A. M. (2005) Functional characterization of a Na^+-coupled dicarboxylate carrier protein from *Staphylococcus aureus*. *J. Bacteriol. 187*, 5189−5194.

(4) Hall, J. A., and Pajor, A. M. (2007) Functional reconstitution of SdcS, a Na^+-coupled dicarboxylate carrier protein from *Staphylococcus aureus*. *J. Bacteriol. 189*, 880−885.

(5) Mancusso, R., Gregorio, G. G., Liu, Q., and Wang, D. N. (2012) Structure and mechanism of a bacterial sodium-dependent dicarboxylate transporter. *Nature 491*, 622−627.

(6) Krishnamurthy, H., Piscitelli, C. L., and Gouaux, E. (2009) Unlocking the molecular secrets of sodium-coupled transporters. *Nature 459*, 347−355.

(7) Pajor, A. M., and Randolph, K. M. (2007) Inhibition of the Na^+/dicarboxylate cotransporter by anthranilic acid derivatives. *Mol. Pharmacol. 72*, 1330−1336.

(8) Pajor, A. M., and Sun, N. (1996) Functional differences between rabbit and human Na^+-dicarboxylate cotransporters, NaDC-1 and hNaDC-1. *Am. J. Physiol. 271*, F1093−F1099.

(9) Joshi, A. D., and Pajor, A. M. (2009) Identification of Conformationally Sensitive Amino Acids in the Na^+/Dicarboxylate Symporter (SdcS). *Biochemistry 48*, 3017−3024.

(10) Pajor, A. M., and Sun, N. N. (2010) Single nucleotide polymorphisms in the human Na^+-dicarboxylate cotransporter affect transport activity and protein expression. *Am. J. Physiol. 299*, F704−F711.

(11) Bulling, S., Schicker, K., Zhang, Y. W., Steinkellner, T., Stockner, T., Gruber, C. W., Boehm, S., Freissmuth, M., Rudnick, G., Sitte, H. H., and Sandtner, W. (2012) The mechanistic basis for noncompetitive ibogaine inhibition of serotonin and dopamine transporters. *J. Biol. Chem. 287*, 18524−18534.

(12) Zhao, Z. G., Zhang, M., Zeng, X. M., Fei, X. W., Liu, L. Y., Zhang, Z. H., and Mei, Y. A. (2007) Flufenamic acid bi-directionally modulates the transient outward K^+ current in rat cerebellar granule cells. *J. Pharmacol. Exp. Ther. 322*, 195−204.

(13) Pajor, A. M., and Randolph, K. M. (2005) Conformationally sensitive residues in extracellular loop 5 of the Na^+/dicarboxylate cotransporter. *J. Biol. Chem. 280*, 18728−18735.

(14) White, M. M., and Aylwyn, M. (1990) Niflumic and flufenamic acids are potent reversible blockers of Ca^{2+}-activated Cl^- channels in *Xenopus* oocytes. *Mol. Pharmacol. 37*, 720−724.

(15) Konrad, R. J., Jolly, Y. C., Major, C., and Wolf, B. A. (1992) Inhibition of phospholipase A2 and insulin secretion in pancreatic islets. *Biochim. Biophys. Acta 1135*, 215−220.

(16) Basketter, D. A., and Widdas, W. F. (1978) Asymmetry of the hexose transfer system in human erythrocytes. Comparison of the effects of cytochalasin B, phloretin and maltose as competitive inhibitors. *J. Physiol. 278*, 389−401.

(17) Carruthers, A., and Helgerson, A. L. (1991) Inhibitions of sugar transport produced by ligands binding at opposite sides of the membrane. Evidence for simultaneous occupation of the carrier by maltose and cytochalasin B. *Biochemistry 30*, 3907−3915.

(18) Buchanan, B. B., Eiermann, W., Riccio, P., Aquila, H., and Klingenberg, M. (1976) Antibody evidence for different conformational states of ADP, ATP translocator protein isolated from mitochondria. *Proc. Natl. Acad. Sci. U.S.A. 73*, 2280−2284.

(19) Zhou, Z., Zhen, J., Karpowich, N. K., Goetz, R. M., Law, C. J., Reith, M. E., and Wang, D. N. (2007) LeuT-desipramine structure reveals how antidepressants block neurotransmitter reuptake. *Science 317*, 1390−1393.

(20) Singh, S. K., Yamashita, A., and Gouaux, E. (2007) Antidepressant binding site in a bacterial homologue of neurotransmitter transporters. *Nature 448*, 952−956.

(21) Segel, I. H. (1975) *Enzyme kinetics*, John Wiley and Sons, New York.

(22) Hamill, S., Cloherty, E. K., and Carruthers, A. (1999) The human erythrocyte sugar transporter presents two sugar import sites. *Biochemistry 38*, 16974−16983.

(23) Schulze, S., Koster, S., Geldmacher, U., Terwisscha van Scheltinga, A. C., and Kuhlbrandt, W. (2010) Structural basis of

Na^+-independent and cooperative substrate/product antiport in CaiT. *Nature 467*, 233−236.
(24) Reyes, N., and Tavoulari, S. (2011) To be, or not to be two sites: That is the question about LeuT substrate binding. *J. Gen. Physiol. 138*, 467−471.
(25) Quick, M., Shi, L., Zehnpfennig, B., Weinstein, H., and Javitch, J. A. (2012) Experimental conditions can obscure the second high-affinity site in LeuT. *Nat. Struct. Mol. Biol. 19*, 207−211.